

# Estimating ski orientation using IMUs in alpine skiing

Chris Hummel<sup>\*1</sup>, Andreas Huber<sup>2</sup>, Peter Spitzenpfeil<sup>1</sup>

<sup>1</sup> Applied Sport Science, Department Health and Sport Sciences, Technical University of Munich, Munich, Germany

<sup>2</sup> Olympiastützpunkt Bayern, Munich, Germany

\* chris.hummel@tum.de

## ORIGINAL ARTICLE

Submitted: 21 May 2023

Accepted: 22 November 2023

Published: 2 May 2024

### Editor-in-Chief:

Claudio R. Nigg, University of Bern, Switzerland

### Guest Editors:

Thomas Stöggl, Paris Lodron University Salzburg, Austria; Red Bull Athlete Performance Center, Austria

Hermann Schwameder, Paris Lodron University Salzburg, Austria

Hans-Peter Wiesinger, Paris Lodron University Salzburg, Austria

## ABSTRACT

Ski-snow interaction is the essential component of alpine skiing. To understand how a skier manipulates his ski to turn, we need to develop methods to measure the orientation of the ski throughout a complete run. Recent studies tried to use IMUs to estimate edge angle (EA) during skiing.

We introduce and validate a method on how to calibrate and employ IMUs to precisely and accurately measure roll angles (RA) as a matter of changing orientation of the ski around its longitudinal axis in 3D space during skiing.

Static orientation measurements on an inclined plane perfectly correlate ( $r^2 = 1$ ) with 3D motion capturing: RMSE =  $0.18^\circ$  and  $0.24^\circ$  respectively. Bland Altman showed a mean bias of  $0.23^\circ$  (95% CI:  $-0.16^\circ$ ,  $0.63^\circ$ ) and  $0.21^\circ$  (95% CI:  $-0.3^\circ$ ,  $0.73^\circ$ ). Accuracy and drift tests against constant standardised rotational velocities showed no drift behaviour over time, but RA estimation accuracy is reduced with increasing angular velocities ( $SD @ \pm 300^\circ/s$ :  $0.57^\circ$ , max. difference from average at  $\pm 300^\circ/s$ :  $2.7^\circ$ ). During skiing on a ski ergometer the comparison of maximum RA against Vicon showed a mean bias of  $0.13^\circ$  (95% CI:  $-0.86^\circ$  to  $1.1^\circ$ ).

Even though ski ergometer skiing has a similar frequency and angular velocity profile like outdoor skiing, there are more rotational degrees of freedom in outdoor skiing. The foundation is provided in this paper. To understand how a skier manipulates the ski on snow and to understand RA and EA progression during a turn in detail, further research should validate the method in the field and additionally look into RA progression within individual turns.

### Keywords

*edge angle, roll angle, ski-snow interaction, inertial measurement units, validation, Madgwick filter*

## Citation:

Hummel, C., Huber, A., & Spitzenpfeil, P. (2024). Estimating ski orientation using IMUs in alpine skiing. *Current Issues in Sport Science*, 9(3), Article 004. <https://doi.org/10.36950/2024.3ciss004>

## Introduction

Ski-snow interaction is an essential aspect of competitive and recreational skiing. To perform a turn, a skier changes the orientation and the loading pattern of the ski to generate a reaction force that leads to a redirection (Reid et al., 2020). Due to the shape of modern skis, a skier mainly manipulates the ski's orientation around two axes to turn: around the longitudinal axis to change the edge angle (EA) and by manipulating the vertical axis (heading) of the ski, which changes the angle of attack (AA; Lieu & Mote, 1985).

Currently, methods to measure ski orientation during skiing are limited to either a small area (Reid et al., 2020) using 3D kinematic systems or to indoor skiing on a treadmill using IMUs (Snyder et al., 2022). However, 3D kinematic systems are complex to set up and time demanding in post-processing. A recent study demonstrated the estimation of EAs with the application of inertial measurement units (IMU) at the back of the ski boots (Snyder et al., 2020). IMUs have many advantages over motion capture systems, as they are small, wearable, affordable and can easily be used outside the laboratory (van Dijk et al., 2021). While IMUs can be used to calculate the global orientation of objects they are attached to, the reference to the snow surface is more relevant to understand ski-snow interaction (e.g. radial forces, groove formation, ski deflection or torsion; Federolf et al., 2010; Snyder et al., 2021; Thorwartl et al., 2023) and the turning technique of a skier. Gilgien et al. (2013) proposed a method to model the snow surface by triangulating survey points of a differential Global Navigation Satellite System, which could be used to calculate the orientation of the ski relative to the local snow surface. While edge angle is a well-established term to describe the angle between the ski and the hill surface

about the longitudinal axis, there is no uniform term regarding the orientation of the ski in 3D-space. We suggest using roll angle (RA) of the ski to be in accordance with aircraft principal axes, as in a recent publication by Thorwartl et al. (2023).

In general, a six-axis IMU consists of an accelerometer (ACC) and a gyroscope (GYRO), which measure linear acceleration and angular velocity along three orthogonal axes. Orientation is not measured directly, but by determining an initial state and integration of the angular velocity. During this process, sensor noise and sensor offset lead to sensor drift over time and therefore errors in the estimation of the orientation (Bergamini et al., 2014). Several techniques are applied to cope with drift: correction of the sensor's orientation from cyclic movement pattern in which the orientation is known from time to time (Zandbergen et al., 2022), or the use of information from further sensors like magnetometer (Bergamini et al., 2014) or global navigation satellite system (GNSS; Brodie et al., 2008; Fasel et al., 2016). The Madgwick filter (Madgwick et al., 2011) is a common filter used in human motion tracking (van Dijk et al., 2022). It employs numerical integration of GYRO data to deduce an attitude. Additionally, it employs a gradient descent algorithm to optimize the attitude estimations using information from the ACC. While gyroscope-derived attitude estimations allow the capturing of dynamic and high-speed motions over brief intervals, incorporating directional indications derived from the ACC allow for long-term drift compensation (Madgwick et al., 2011). The advantage of the Madgwick filter, with its complementary characteristics, is to be responsive to high angular velocities, while being resistant to drift over time.

Pilot tests during slalom skiing showed that the Madgwick filter performs well in estimating plausible RA (not validated) in recreational skiers with angular velocities of up to  $250^\circ/\text{s}$  as well as in young elite slalom skiers ( $350^\circ/\text{s}$ ). Therefore, this study aims to present a detailed description of the used method and validate the applicability of the Madgwick filter to estimate RA, especially peak RA, in alpine skiing.

## Methods

The method section first discusses the relevant coordinate systems to measure RA and EA. Next, the transformation between coordinate systems is explained. In literature there seems to be some unclarity in this regard, e.g. the interchangeable use of IMU and ski coordinate systems and global and local coordinate systems. Afterwards, we present the current method and steps to validate it.

### Reference systems

To determine the ski's orientation, the definition of the reference coordinate systems, the corresponding rotational axes and the definition of the angles are important. The global reference coordinate system (Figure 1, A) is defined by the  $Z_G$  axis which points against earth's

gravity-vector. The  $Y_G$  axis is aligned with the initial position of the ski's longitudinal axis (from tail to tip of the ski, usually along the fall line) and is perpendicular to  $Z_G$ . Finally,  $X_G$  is defined perpendicular to the other two axes. Rotation directions are defined according to the right-hand rule. The ski-bound coordinate system (Figure 1, B) originates at the ski's centre point, with the  $Y_S$  axis aligning with the longitudinal axis of the ski (tail to tip).  $X_S$  axis pointing towards the right side of the ski perpendicular to  $Y_S$  along the local snow surface and the  $Z_S$  axis pointing upward, perpendicular to  $X_S$  and  $Y_S$ . The ski's orientation is described by Euler angles. RA is defined as the Euler angle resulting from a rotation around the  $Y_G$  axis by which the ski's coordinate system is achieved. Respectively, pitch is defined as rotation around the  $X_G$  axis and yaw as rotation around the  $Z_G$  axis. Finally, the local coordinate system is relevant to retrieve EA and is dependent on the ski's centre point. It is a variation of the global coordinate system rotated about the global  $X_G$  and  $Y_G$  axes. Hereby, the  $X_L$ - $Y_L$  plane is locally matched with the snow surface (Figure 1, C). Figure 1 also shows an example of the difference between RA  $\gamma$  with the global reference while the EA  $\theta$  is defined in reference to the local reference.

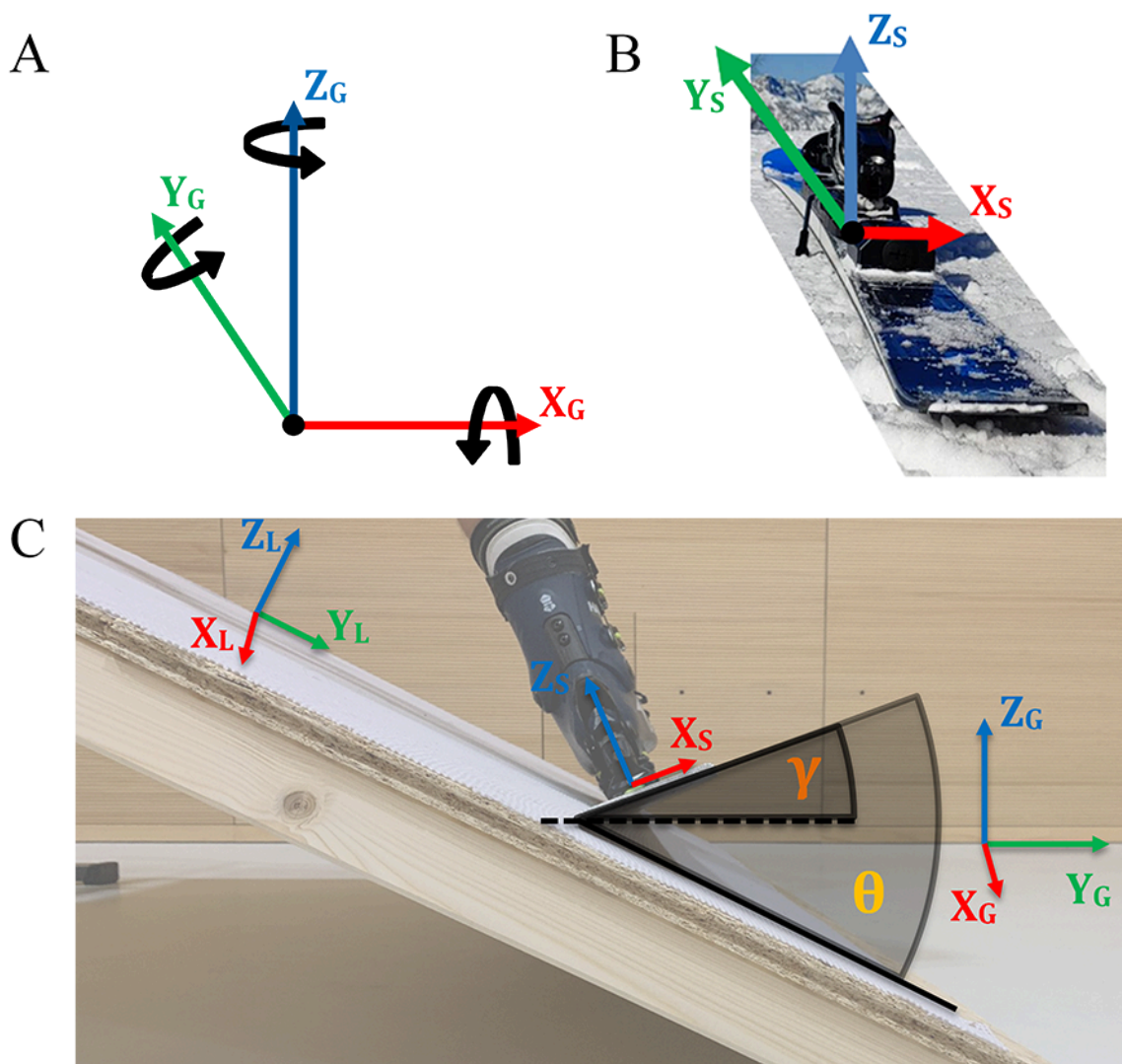


**Figure 1** Definition of the orientations of **A** global ( $X_G$   $Y_G$   $Z_G$ ) coordinate system including rotation directions, **B** the ski ( $X_S$   $Y_S$   $Z_S$ ) coordinate system, **C** local ( $X_L$   $Y_L$   $Z_L$ ) coordinate systems in a skiing situation. **C** also shows the difference between roll angle ( $\gamma$ , orange) and its definition against the horizontal plane of the global reference system and edge angle ( $\theta$ , yellow) with the definition against the local coordinate system. X axes are depicted in red, Y axes in green and Z axes in blue.

**Mounting offset and initial orientation offset**

A relation between the IMU coordinate system and the reference coordinate systems must be established to determine the ski’s orientation. Relations are defined

in two steps to be able to distinguish between mounting and initial orientation offset. This allows for non-level surfaces as initial positions before a trial. The mounting offset establishes the relation between the IMU coordinate system and the ski’s coordinate system. It is obtained by placing the ski or the ski boot on a flat

and level surface. From the accelerometer readings, the current roll ( $\gamma$ ) and pitch angles ( $\beta$ ) are retrieved using equations 1 and 2, with  $A$  being the acceleration along the specified axes:

$$\gamma = \arctan2(A_x, A_z) \quad (1)$$

$$\beta = \arctan2\left(-A_y, \sqrt{A_x^2 + A_z^2}\right) \quad (2)$$

The initial orientation offset relates the ski's coordinate system to the global coordinate system and is determined during a zero-movement phase directly before the start of a trial. Yaw is arbitrarily set to zero, as neither GNSS nor a magnetometer is used to correct the heading.

## Study design

Before evaluating the applicability and quality of the method, the individual steps of the current measurement procedure with regard to their contribution to RA estimation are described. Afterwards, the first experiment evaluates the global orientation in a static scenario, which is relevant for the relation between the individual reference systems. The second experiment evaluates the RA estimation validity of the filter at different angular velocities. The third experiment evaluates the algorithm in a complex skiing-like movement in a lab setting.

## Current measurement procedure

This section describes our current procedure to measure RA on the skiing hill. Before mounting, the first step is the calibration of the IMU, the necessary steps are presented in the next section. After calibration, the IMU is attached to the subject's ski boot and placed on a level surface to retrieve the mounting offset. The subject puts the boot on and moves to the starting point. Before each run, there is a phase of standing still for five seconds (zero-movement phase) to retrieve

the initial orientation offset and the GYRO offset. After the run, ACC and GYRO data are retrieved from the data logger. We observed high frequency noise when recording ACC and GYRO readings at rest, which should be removed before applying the Madgwick filter. Redhyka et al. (2015) suggest the use of moving average, Savitzky-Golay or Kalman filters to reduce noise in IMU data, additionally low-pass filters were included in our testing. Their performances in the power spectrum density analysis in a resting as well as simulated skiing situation made it obvious that the moving average performed best attenuating unwanted high frequencies. To reduce the risk of changing peak angle values and keep the dynamic of the signal, we choose a small window of 10 samples to preserve as much of the signal as possible. The filtered data is passed through the Madgwick filter, followed by applying the offsets. Results are reported back to the subject.

## Calibration of the IMU

The IMU (2D Debus & Diebold Meßsysteme GmbH, Karlsruhe, GER) is powered for one hour to allow the electronics to reach constant temperatures before calibrating and measuring. The calibration of ACC and GYRO takes four steps, the first two are only performed once before the study:

1. Sensor and housing are aligned using built-in coordinate transformation in WinIt (2D Debus & Diebold Meßsysteme GmbH).
2. The IMU is attached to the rotatory head of an isokinetic strength measurement device (Isomed 2000, D. & R. Ferstl GmbH, Hemau, GER) along each axis and turned with an angular velocity of  $\pm 50$ ,  $\pm 100$ ,  $\pm 150$ ,  $\pm 200$  and  $\pm 300^\circ/\text{s}$  for one minute. The averages of the IMU readings during the constant rotational velocity phase are compared against the set angular velocities. Resulting linear regression models (LRMs) are applied to the GYRO data of all measurements.

Step three is performed before each measurement day and step four before every trial:



3. IMU scaling calibration: The three axes of the IMU are aligned 0°, 30°, 60° and 90° along and against the g-vector using a 3D printed calibration tool. ACC readings are averaged over one second for every orientation and compared against theoretical values. Received LRMs are applied to all measurements of the respective day in post processing.
4. GYRO offset is determined individually for each axis during the zero-movement phase before each measurement. For each zero-movement phase the moving standard deviation (window length: 0.5 s) is calculated to determine the steadiest phase. The steadiest time window is averaged and subtracted as GYRO offset of the corresponding measurements.

### Experiment 1: Inclined plane in static situation, IMU positioning

The measurement setup is visualized in Figure 2. One subject is placed on an inclined plane at three different slope angles (flat: 0°, middle: 12.4°, steep: 26.7°), which are selected to be within the range of gradient stated in the regulations for slalom alpine ski racing (International Ski Federation FIS, 2020). At each slope the ski is edged at four angles (0°, 10°, 20°, 30°) for four different yaw angles (0°, 30°, 60°, 90°). The yaw angle is achieved by orienting the ski along marks on the plane, next EA is generated by inducing an angle specific wedge between the plane and ski centre to take position. After position is reached, the wedge is removed while the subject remains in this position for five seconds. The global orientation is measured by one IMU ( $\pm 16$  g,  $\pm 2000^\circ/\text{s}$ , 1600 Hz, 1000 Hz ODR, 16-bit ADC) mounted to the right ski boot, while a second is mounted to the right ski's surface. Every IMU is rigidly connected to three markers (14 mm), which are tracked by an eight camera motion capture system (100 Hz, Vicon, Vicon Motion Systems Ltd., Oxford, UK). Overall, three repetition measurements of all positions

are performed. The experiment addresses the precision of the static orientation estimation from ACC readings. Further, the question regarding IMU positioning to calculate RA is addressed. Linear regressions and Bland-Altman plots (Bland & Altman, 1986) compare the accuracy of the static orientation calculation from Vicon (gold standard) to the IMU. Finally, RA differences between the sensor positions are compared using the marker information, to evaluate the sensor positioning.

### Experiment 2: Standardized rotation velocity

In the second experiment both IMUs are stacked and attached to the rotational arm of an isokinetic strength measurement device, the rotational axis is hereby consecutively aligned with the sensor rotational axes in three setups. Angular velocity is set to  $\pm 50$ ,  $\pm 100$ ,  $\pm 150$ ,  $\pm 200$  and  $\pm 300$  /s for one minute duration with a movement range of 220° (absolute end points: -50° to 170°) without static phases between direction changes. Five trials were performed for each setup and each velocity. Each trial started with a five second zero-movement phase. The precision and accuracy of the filter ( $\beta = 0.8$ ) with regard to angular velocity is derived from the standard deviation at the minimum (-50°) and maximum (170°) end point for each angular velocity. To account for misalignment of the IMU-axis concerning the rotatory axis, the mean of the respective minimum and maximum angles measured by the IMU is used as reference, instead of the absolute angles. Automatic peak angle detection is performed using Matlab (R2022b, MathWorks, Natick, MA, USA) with a 10-samples moving average filter.

To assess drift the confidence interval of the slope component of linear regressions are considered. The indices of consecutive end points (including minimum and maximum) are used as x-values, while the y-values consist of the differences between the respective mean value and the corresponding measured angle. A drift would be visible in maximum and minimum end-point equally. By utilizing the difference, a single metric can be used to assess drift.

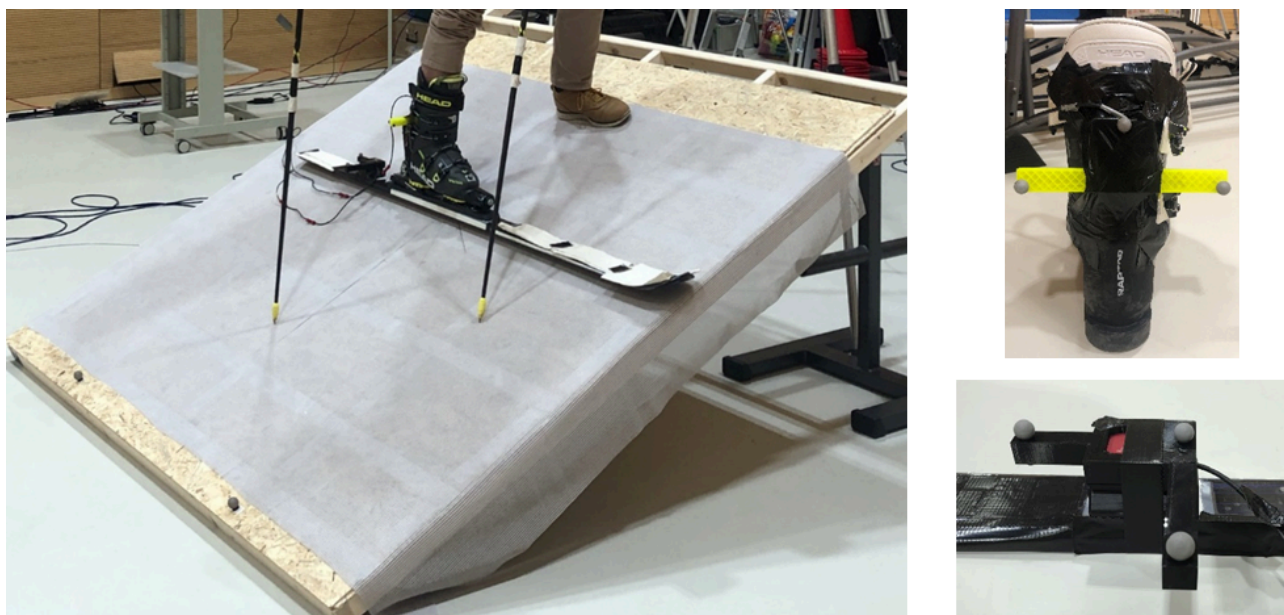


**Figure 2** The setup for the inclined plane experiment. A wooden plane is placed at an angle on the plane marks for the centre point and the yaw positions are marked. Right side shows the 3D printed housings the IMUs are enclosed in attached to the right boot and the top of the right ski. To both housings 3 markers are attached to create a coordinate system that aligns with the IMU coordinate system.

### Experiment 3: Complex movement on the Skier's Edge

Six subjects (3 female, 3 male) performed three trials of simulated skiing on a Skier's Edge (Skier's Edge Company, Utah, USA) each. Mounting offset was determined for each subject prior and every trial started with a zero-movement phase for GYRO offset and initial position offset. Trial duration was set to one minute to match the duration of a slalom race. IMU and Vicon markers (14 mm) were attached to the platform of the right boot (Figure 3). Vicon measurement

frequency was set to 200 Hz for this experiment. Four markers were used to compensate for potentially covered markers. In case of reconstruction rigid body properties were used. First the calibration is applied to the IMU raw data, afterwards it is filtered using a 10-samples moving average filter and the Madgwick filter is applied. Minimum and maximum angles with a minimum prominence of  $15^\circ$  are automatically detected and matched between both systems. Matched angles are compared using regression and Bland-Altman.



**Figure 3** The Skier's Edge with four markers (red arrows) attached to the right platform and the IMU (green arrow) mounted vertically under the rotation joint.

To evaluate if Skier's Edge skiing and outdoor skiing can be compared regarding angular movement profiles, for each trial the maximum angular velocity and average movement frequency were determined, averaged and reported. Typical skiing frequencies are between 0.69 Hz and 1.11 Hz according to Spörri et al. (2016). Skiing frequency  $f_{ski}$  is determined for each trial by:

$$f_{ski} = \frac{n_{turns} - 1}{(t_n - t_1)} \quad (3)$$

Where  $n$  is the total number of turns,  $t$  is the time in seconds of the specified turn.

### Statistical consideration

All statistical analysis were performed using Matlab (R2022b). For linear regression models sample size, root mean square error (RMSE), the equation and  $r^2$  is reported. Vicon is used as reference method (gold standard), thus the differences of both measurement systems

are compared against the Vicon measurements in the Bland Altman analysis (Bland & Altman, 2003). Standard deviation ( $SD$ ), mean and  $\pm 1.96 * SD$  are reported, to quantify the agreement of both systems. Systematic bias is optically assessed from the Bland-Altman plots and a fixed bias is detected if the 95% CI of the differences of both systems does not include  $0^\circ$  (Ludbrook, 2002). In accordance, if the 95% CI of the slope parameter for the drift detection does not include zero, the individual trial is rated as drifting. Alpha was set to 0.05 for all tests. For readability, values are rounded to two decimals.

## Results

### Inclined plane

A total of 144 data points from three sets of 16 orientations and three inclinations were captured per mounting position. Figure 4 shows the regression of the RA for the IMU mounted to the right ski (blue) and the IMU mounted to the right boot (red).



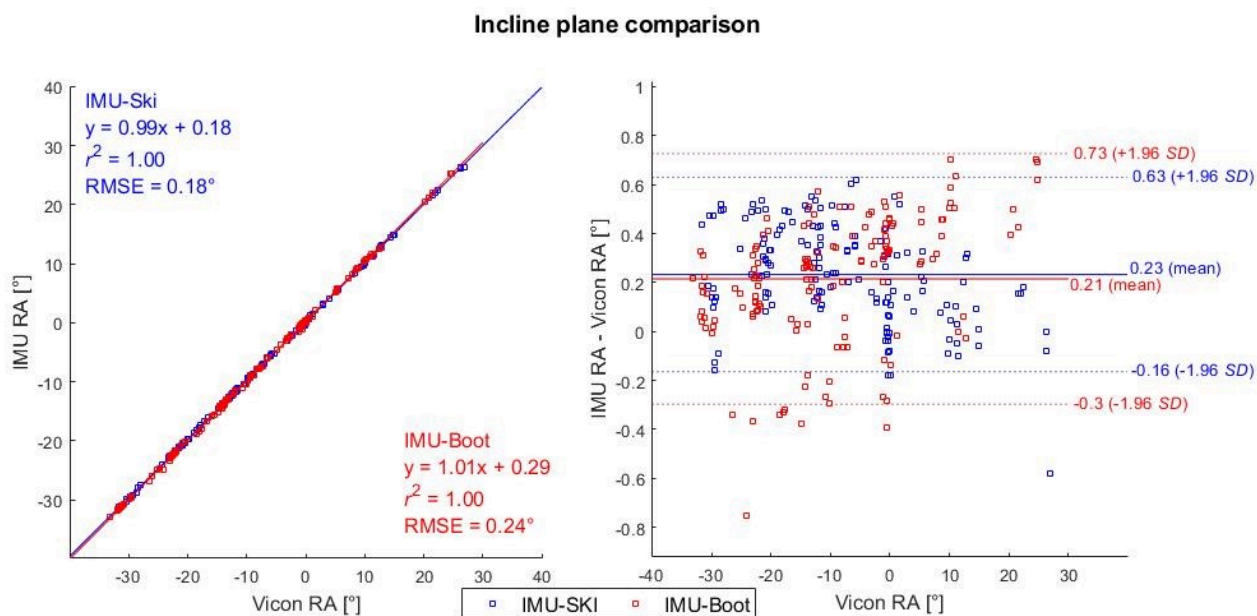


**Figure 4** Results from the inclined plane experiment. Left graph shows the correlation analysis and the right graph the Bland Altman plot including mean difference and 95% CI as dashed lines. Data retrieved from the IMU and markers attached to the ski are presented in blue. Data from the IMU and markers attached to the boot are presented in red.

**Table 1**

Difference in RA between the boot and the ski mounting position within the inclined plane experiment.

Pitch condition	Yaw	Roll			
		0°	10°	20°	30°
<i>flat</i>	0°	0.00°	1.36°	1.30°	1.36°
	30°	-0.10°	1.53°	1.53°	1.50°
	60°	-0.09°	1.37°	1.49°	1.81°
	90°	0.00°	1.41°	1.53°	1.29°
<i>middle</i>	0°	0.00°	1.23°	1.21°	1.07°
	30°	0.08°	1.54°	1.43°	1.43°
	60°	0.67°	2.21°	2.06°	1.82°
<i>steep</i>	0°	0.00°	0.83°	0.79°	0.81°
	30	0.31°	1.43°	1.23°	1.04°
	60	0.97°	2.96°	2.24°	2.06°
	90	1.67°	3.99°	3.51°	3.03°

The ski-mounted IMU regression equation is  $y = 0.99x + 0.18$  ( $r^2 = 1$ ) with a RMSE of  $0.18^\circ$ . The Bland-Altman plot shows a mean bias of the IMU method of  $0.23^\circ$  towards the Vicon system, where 95% of all values lay within  $0.79^\circ$  ( $SD = 0.2^\circ$ ).  $0^\circ$  is included in the 95% CI. The equation describing correlation between the IMU mounted to the ski boot is  $y = 1.01x + 0.29$  ( $r^2 = 1$ ) with an RSME of  $0.24^\circ$ . The mean bias is  $0.23^\circ$  towards Vicon and 95% of all values lay within  $1.03^\circ$  ( $SD = 0.26^\circ$ ).

Table 1 shows the mean RA differences over the three sets between the ski-mounted IMU and the boot-mounted IMU calculated from Vicon data. On a flat plane RA difference increases when any EA position other than  $0^\circ$  is taken. At the middle pitch condition RA differences tend to increase above  $0^\circ$  EA as well as from top to bottom (for increasing yaw angles). The same is true for the steep condition: maximum differences ( $3.99^\circ$  and  $3.51^\circ$ ) are reached when standing

perpendicular to the fall line ( $90^\circ$  yaw) at  $10^\circ$  and  $20^\circ$  EA.

### Standardized rotation velocity

It appears that the precision of the Madgwick filter becomes worse in estimating RA with increasing angular velocities (Figure 5). While the standard deviation stays within  $0.57^\circ$  up until  $300^\circ/s$  rotational velocity, occasionally extreme values differ further from the mean estimation. For context, IMU 1 was mounted to the ski, while IMU 2 was mounted to the ski boot in the previous experiment. At  $300^\circ/s$  all values stay within a range of  $2.7^\circ$ .

Evaluating drift behaviour over movement cycles by looking at the 95% CIs of the slope parameter, 6 out of 75 trials did not include 0, four trials at  $200^\circ/s$ , one at  $50^\circ/s$  and one at  $300^\circ/s$  for IMU 1 and 4 out of 75 trials for IMU 2, 2 trials at  $50^\circ/s$ , one each at  $100^\circ/s$  and  $300^\circ/s$ .

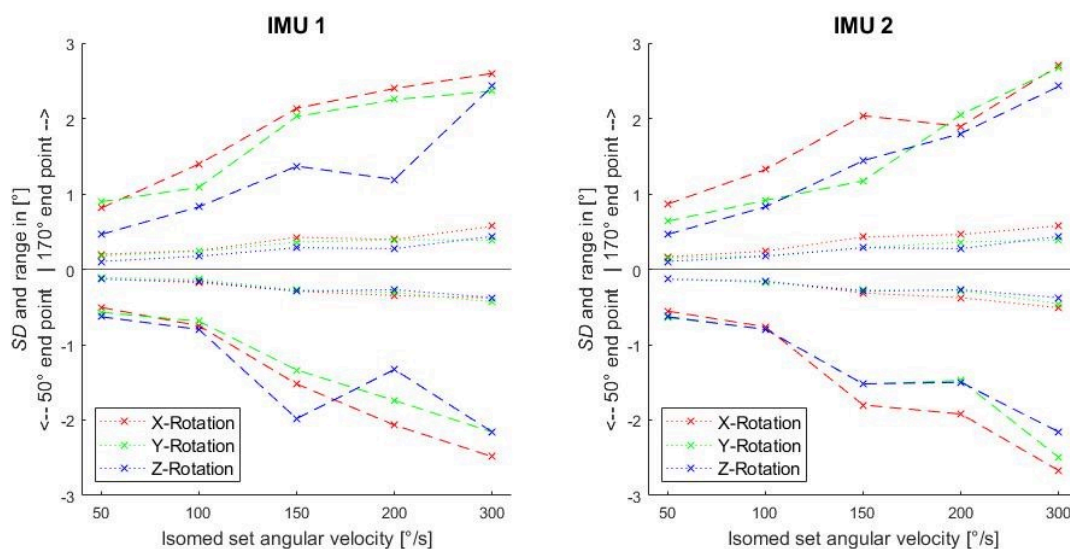


**Figure 5** SD and range around mean measured value for predefined angular velocities. Dotted line indicates standard deviations, dashed lines ranges. Values for the endpoint at  $170^\circ$  are displayed on the positive axis while values for the  $50^\circ$  endpoint are displayed negatively. Red represents rotation about the X axis of the IMU, respectively green for the Y axis and blue for the Z axis.

### Complex movement on the Skier's Edge

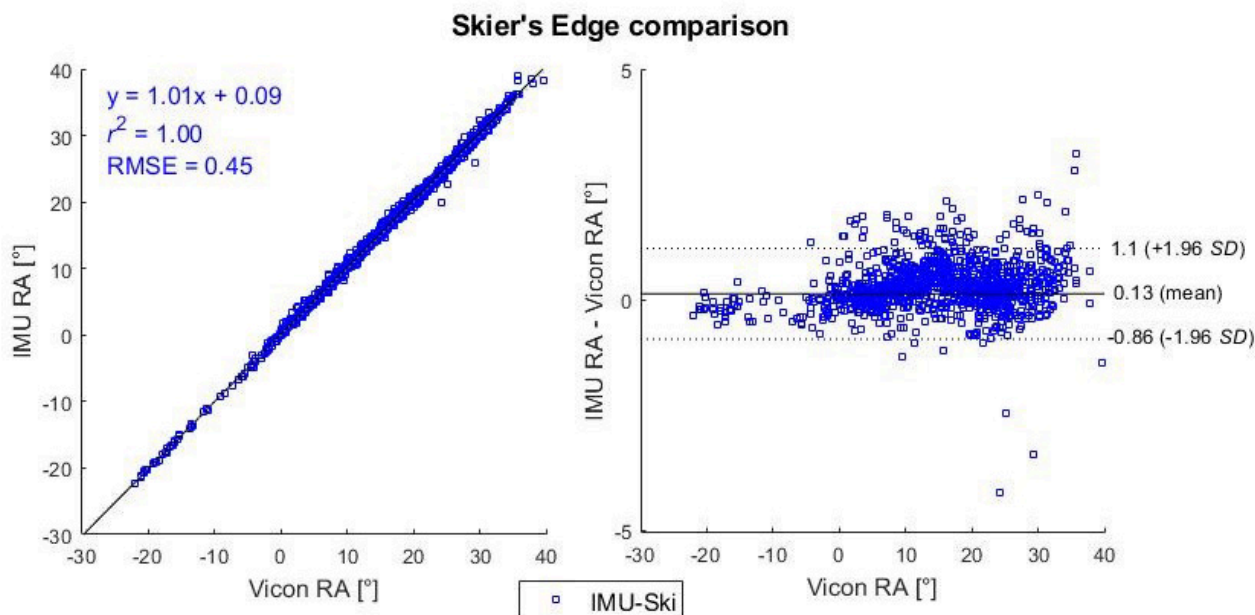


**Figure 6** Results for the Skier's Edge measurement. Left graph displays the correlation between Vicon and IMU RAs. Right graph shows the difference between Vicon and IMU RAs with regard to the RA from Vicon as reference system. The mean is displayed with dotted lines indicating the 95% CI.

For the validation of the IMU system with Vicon, 1,700 turns were taken into consideration (Figure 6). Results from the first experiment show that only the IMU mounted to the ski can accurately determine RA, therefore only its location was considered for analysis. Regression analysis returns the equation  $y = 1.01x + 0.09$  with an RMSE of  $0.45^\circ$  and  $r^2 = 1.00$ . Bland-Altman shows a mean bias of the IMU system of  $0.13^\circ$

with the 95% CI ranges from  $-0.86^\circ$  to  $1.1^\circ$  including  $0^\circ$ . No systematic bias is recognized from the Bland Altman plot. Subjects "skied" on average with a frequency of 0.98 Hz, with an average maximum angular velocity of  $263^\circ/s$  (Table 2). From these numbers, skiing on snow and Skier's Edge skiing show similar patterns regarding the angular movement profile around the roll axis.

**Table 2**

Average skiing frequency and maximum angular velocity for individual subjects over three trials.

Subject	Average skiing frequency [Hz]	Average maximum angular velocity [°/s]
1	0.89	220.48
2	0.95	210.09
3	0.92	246.71
4	1.06	345.96

Subject	Average skiing frequency [Hz]	Average maximum angular velocity [°/s]
5	1.06	267.46
6	1.01	292.89

## Discussion and conclusion

The goal of this study was to propose a method that validly estimates peak RA during alpine skiing. The main finding was that by carefully calibrating the IMU and applying the Madgwick filter IMUs can be used to estimate RA during skiing. Others reported for their method also validated on a ski ergometer (Snyder et al., 2020) a limit of agreement (LOA) of  $\pm 4.37^\circ$  for maximum EA. This method showed a higher precision and accuracy with 95% of the values being within  $1.96^\circ$  of the gold standard's reference.

A well-calibrated IMU is a requirement for accurate orientation measurements: A small gyroscope offset can largely affect the result of the integration. While the sensor-housing offset and GYRO scaling appear to be constant for long durations, it is unclear how often the ACC needs recalibration as throughout the study the ACC calibrations differed between days but stayed in a similar range. GYRO offset appeared to be very volatile, making it necessary to calibrate close to the actual trials. The mean biases in all experiments are not of concern and can likely be attributed to misalignment of markers and IMU in the 3D printed enclosure. Overall, the referencing of the IMU coordinate system to the ski and global coordinate system are highly dependent on an accurate and precise determination of the IMUs global orientation. With an accuracy of  $1.03^\circ$  (95% CI) the demand for accurate referencing is satisfied.

The standardised rotation test showed that the estimation of individual RAs ranges up to  $2.7^\circ$  and gave an idea of the magnitude of accuracy at different rotational velocities. While some trials showed drift, there is no pattern of systematic drift over time not even for higher angular velocities, meaning the Madgwick filter

is able to compensate inaccuracies even during highly dynamic movements. The more meaningful result is that 95% of the values stay within the range of  $\pm 1.13^\circ$  ( $1.96 * SD$ ) of the true value independent of rotational velocity. In the alpine skiing context, angular velocities are not constant over time but alternating, therefore the filter is likely to compensate extreme values quickly in phases with lower angular velocity.

Summarizing the above aspects, the method allows for an accurate measurement of the real orientation of the ski centre in a global reference system. Therefore, this method appears to be applicable in alpine skiing.

A main finding of this study regards the mounting location of the IMU, all studies investigating EA or RA mounted the IMUs to the upper posterior cuff of the ski boot. While this location is well protected and handy, already static measurements on an inclined plane show that there is relative movement between boot and ski of  $3.99^\circ$ , making this location a source of error when the aim is to investigate ski-snow interaction. It is unclear if the relative movement is a result from the bend of the boot or the binding acting as joint between boot and ski. The largest differences in RA were observed at the steepest hill setting with an EA of  $10^\circ$  to  $20^\circ$  at  $90^\circ$  yaw. In this scenario the most force is applied to the longest transversal lever inducing a torque into the ski-boot-binding system. If  $3.99^\circ$  can be observed in a static scenario, a dynamic scenario with additional radial forces could affect the system even more – the error is likely to become even larger. The Skier's Edge setup was not suitable to estimate the error in a dynamic setting, as there is no abutment inducing a counter rotation into the platform-boot system.

Further considerations are to increase the sensor resolutions by reducing the measurement range. A higher resolution reduces the discrete step distance and leads to a more accurate integration. Currently the IMUs are configured to  $\pm 2000^\circ/\text{s}$  and  $\pm 16\text{g}$ , while the highest angular velocity on the Skier's Edge was  $355^\circ/\text{s}$ . Still, leaving head room for the gyroscope makes sense to avoid sensor clipping in outdoor skiing scenarios on icy/bumpy hills. Same is true for the ACC. Depending on the scenario a higher resolution could be advantageous over a wider measurement range.

Even though angular velocity and frequency are comparable between skiing on the Skier's Edge and outdoor, outdoor skiing contains further pitfalls (e.g. impacts, temperature changes, vibrations) that could influence the precision of the Madgwick filter. Skiing on the Skier's Edge limits movement to the lateral axis and roll rotation. Major degrees of freedom relevant to skiing are missing: rotation around the pitch and the yaw axis. However, due to the complementary characteristics the filter might even profit from more movement along and around all three axes. Nevertheless, this speculation is subject to further research.

When willing to investigate turning strategies in athletes, maximum angles are without doubt important. Further, it would be interesting to validate curve progression. This would be of particular interest, to understand strategies for change of edge and yaw angle to perform a turn.

### Potential applications

The determination of the ski's orientation using IMUs allow outdoor measurements on a larger area compared to a 3D kinematic system. The method described in this paper helps to understand ski-snow interaction and the ski mechanics to answer the question how a ski bends during a turn and the role of torsion during skiing (Spitzenpfeil et al., 2023). Further, it could be used as a training tool for elite athletes. The Madgwick filter has a low computational demand and therefore can be applied in real-time within a training setting to give athletes feedback about their turning strategies for individual turns. Additionally, it can be used to

improve performance in ski cross due to feedback of the loading patterns in pump track sections.

## References

- Bergamini, E., Ligorio, G., Summa, A., Vannozzi, G., Capozzo, A., & Sabatini, A. M. (2014). Estimating orientation using magnetic and inertial sensors and different sensor fusion approaches: Accuracy assessment in manual and locomotion tasks. *Sensors*, *14*(10), 18625–18649. <https://doi.org/10.3390/s141018625>
- Bland, J. M., & Altman, D. G. (1986). Statistical methods for assessing agreement between two methods of clinical measurement. *Lancet*, *327*(8476), 307–310. [https://doi.org/10.1016/S0140-6736\(86\)90837-8](https://doi.org/10.1016/S0140-6736(86)90837-8)
- Bland, J. M., & Altman, D. G. (2003). Applying the right statistics: Analyses of measurement studies. *Ultrasound Obstet Gynecol*, *22*(1), 85–93. <https://doi.org/10.1002/uog.122>
- Brodie, M., Walmsley, A., & Page, W. (2008). Fusion motion capture: A prototype system using inertial measurement units and GPS for the biomechanical analysis of ski racing. *Sports Technology*, *1*(1), 17–28. <https://doi.org/10.1080/19346182.2008.9648447>
- Fasel, B., Spörri, J., Gilgien, M., Boffi, G., Chardonens, J., Müller, E., & Aminian, K. (2016). Three-dimensional body and centre of mass kinematics in alpine ski racing using differential GNSS and inertial sensors. *Remote Sensing*, *8*(8), Article 671. <https://doi.org/10.3390/rs8080671>
- Federolf, P., Roos, M., Lüthi, A., & Dual, J. (2010). Finite element simulation of the ski–snow interaction of an alpine ski in a carved turn. *Sports Engineering*, *12*(3), 123–133. <https://doi.org/10.1007/s12283-010-0038-z>
- Gilgien, M., Spörri, J., Chardonens, J., Kröll, J., & Müller, E. (2013). Determination of external forces in alpine skiing using a differential global navigation satellite system. *Sensors*, *13*, 9821–9835. <https://doi.org/10.3390/s130809821>



- International Ski Federation FIS. (2020). *The international ski competition rules (ICR). Book IV. Joint regulations for alpine skiing* (2020th ed.). International Ski Federation FIS. [https://assets.fis-ski.com/image/upload/v1593675483/fis-prod/assets/ICR\\_02072020.pdf](https://assets.fis-ski.com/image/upload/v1593675483/fis-prod/assets/ICR_02072020.pdf)
- Lieu, D., & Mote, C. (1985). Mechanics of the turning snow ski. In R. J. Johnson & C. D. Mote (Eds.), *Skiing trauma and safety: Fifth international symposium* (pp. 117–140). ASTM International. <https://doi.org/10.1520/STP46631S>
- Ludbrook, J. (2002). Statistical techniques for comparing measurers and methods of measurement: A critical review. *Clinical and Experimental Pharmacology and Physiology*, 29(7), 527–536. <https://doi.org/10.1046/j.1440-1681.2002.03686.x>
- Madgwick, S. O. H., Harrison, A. J. L., & Vaidyanathan, R. (2011). Estimation of IMU and MARG orientation using a gradient descent algorithm. *IEEE International Conference on Rehabilitation Robotics*, 1–7. <https://doi.org/10.1109/ICORR.2011.5975346>
- Redhyka, G. G., Setiawan, D., & Soetraprawata, D. (2015). Embedded sensor fusion and moving-average filter for inertial measurement unit (IMU) on the microcontroller-based stabilized platform. *2015 International Conference on Automation, Cognitive Science, Optics, Micro Electro-Mechanical System, and Information Technology (ICACOMIT)*, 72–77. <https://doi.org/10.1109/ICACOMIT.2015.7440178>
- Reid, R. C., Haugen, P., Gilgien, M., Kipp, R. W., & Smith, G. A. (2020). Alpine ski motion characteristics in slalom. *Frontiers in Sports and Active Living*, 2, Article 25. <https://doi.org/10.3389/fspor.2020.00025>
- Snyder, C., Martínez, A., Strutzenberger, G., & Stöggl, T. (2022). Connected skiing: Validation of edge angle and radial force estimation as motion quality parameters during alpine skiing. *European Journal of Sport Science*, 22(10), 1484–1492. <https://doi.org/10.1080/17461391.2021.1970236>
- Snyder, C., Martínez Álvarez, A., Brunauer, R., & Stöggl, T. (2020). Validation of a wearable system for edge angle estimation during alpine skiing. In M. Karzewska-Lindinger, A. Hakkarainen, V. Linnamo, & S. Lindinger (Eds.), *Science and skiing VIII: 8th international congress on science and skiing* (pp. 64–72). Vuokatti Sports Technology Unit of the Faculty of Sport; Health Sciences, University of Jyväskylä.
- Snyder, C., Martínez Álvarez, A., Strutzenberger, G., & Stöggl, T. (2021). Connected skiing: Validation of edge angle and radial force estimation as motion quality parameters during alpine skiing. *European Journal of Sport Science*, 22(10), 1–13. <https://doi.org/10.1080/17461391.2021.1970236>
- Spitzenpfeil, P., Hummel, C., Huber, A., Waibel, K., Menhorn, F., & Senf, B. (2023). Deflection, torsion and edging measurement in alpine skiing. In T. T. Stöggl, H.-P. Wiesinger, & J. Dirnberger (Eds.), *Abstract book of the 9th international congress on science and skiing*. University of Salzburg.
- Spörri, J., Kröll, J., Fasel, B., Aminian, K., & Müller, E. (2016). Course setting as a prevention measure for overuse injuries of the back in alpine ski racing: A kinematic and kinetic study of giant slalom and slalom. *Orthopaedic Journal of Sports Medicine*, 4(2). <https://doi.org/10.1177/2325967116630719>
- Thorwartl, C., Tschepp, A., Lasshofer, M., Holzer, H., Zirkl, M., Hammer, M., Stadlober, B., & Stöggl, T. (2023). Technique-dependent relationship between local ski bending curvature, roll angle and radial force in alpine skiing. *Sensors (Basel)*, 23(8), Article 3997. <https://doi.org/10.3390/s23083997>

- van Dijk, M. P., Kok, M., Berger, M. A. M., Hoozemans, M. J. M., & Veeger, D. H. E. J. (2021). Machine learning to improve orientation estimation in sports situations challenging for inertial sensor use. *Frontiers in Sports and Active Living*, *3*, Article 670263. <https://doi.org/10.3389/fspor.2021.670263>
- van Dijk, M. P., Slikke, R. M. A., Rupf, R., Hoozemans, M. J. M., Berger, M. A. M., & Veeger, D. H. E. J. (2022). Obtaining wheelchair kinematics with one sensor only? The trade-off between number of inertial sensors and accuracy for measuring wheelchair mobility performance in sports. *Journal of Biomechanics*, *130*, Article 110879. <https://doi.org/10.1016/j.jbiomech.2021.110879>
- Zandbergen, M. A., Reenalda, J., Middelaar, R. P., Ferla, R. I., Buurke, J. H., & Veltink, P. H. (2022). Drift-free 3D orientation and displacement estimation for quasi-cyclical movements using one inertial measurement unit: Application to running. *Sensors*, *22*(3), Article 956. <https://www.mdpi.com/1424-8220/22/3/956>

## Acknowledgements

### Funding

The authors thank the German Ski Federation (DSV) for their support.

### Competing interests

The authors have declared that no competing interests exist.

### Data availability statement

All relevant data are within the paper.